

DESIGN ANALYSIS AND 3D MEASUREMENT OF DIFFUSIVE BROADENING IN A Y-MIXER

Ken B. Greiner, Manish Deshpande and John R. Gilbert
Microcosm Technologies, Cambridge, MA 02142

Rustem F. Ismagilov, Abraham D. Stroock and George M. Whitesides
Department of Chemistry and Chemical Biology
Harvard University, Cambridge, MA 02138

Abstract:

Diffusive broadening of a low molecular weight species in pressure driven flow is studied using both experiment and numerical analysis. Confocal microscopy allows experimental visualization of the three dimensional nature of the diffusion. Numerical results support the experimental results, and are used to provide insight into design questions about devices involving diffusive mixing.

Keywords: Diffusion, CAD, Y-mixer, Confocal Microscopy

I. Introduction

The physical phenomenon of diffusive broadening has found many applications in the field of microfluidics. One of the most common is diffusive mixing of chemical or biological compounds, for the purposes of reactions or chemical sensing[1,2]. Others include the study of fast chemical reaction rates at steady state, the fabrication of microelectrodes, and the patterning of various compounds on channel walls [3]. All these applications require a detailed understanding and characterization of the transverse diffusive mixing of two miscible fluids undergoing laminar flow in microchannels.

This work presents results that demonstrate the three dimensional nature of diffusion in pressure driven flows. Experiments using a Y-mixer and a simple reaction were performed, and confocal microscopy was used to visualize the diffusive mixing in three dimensions. These results verify simple theoretical arguments for the scaling of diffusive width with transport length and flow rate. Numerical analysis was used to investigate the effects of diffusive broadening in devices using standard fluorescent microscopy detection systems.

II. Theoretical Analysis

Theoretical arguments to predict the scaling of transverse diffusive width in pressure driven flow have been made by the Harvard University group[4]; a brief summary will be given here. Using dimensional analysis, the thickness of the diffused layer in regions of uniform flow has been found to vary according to $(Dz/U_m)^{1/2}$, where D is the diffusion coefficient, z is the axial distance, and U_m is the flow speed. An extension of the Leveque problem is used to show that the diffused width in regions of shearing flow varies according to $(DHz/U_m)^{1/3}$, where H is the height of the channel.

III. Experiment

We fabricated microfluidic channels using the "rapid prototyping" technique described previously[3]. The channel structure was defined photolithographically in photoresist on a silicon wafer. Poly (dimethylsiloxane) (PDMS) pre-polymer was then cast and cured on this composite wafer / photoresist structure. A PDMS membrane with the negative relief

corresponding to the channel structure was removed from the wafer and sealed to a clean glass cover slip. A syringe pump drove the fluids into the two inlets at a constant flow rate.

We visualized the region of diffusive mixing using confocal fluorescent microscopy (Leica TCS). Fluo-3 is a commercially available, non-fluorescent compound that forms a strongly fluorescent 1:1 complex with a calcium ion ($K_d = 0.39 \mu\text{M}$). The formation of the complex is diffusion-controlled, therefore we could visualize the region of diffusive mixing by

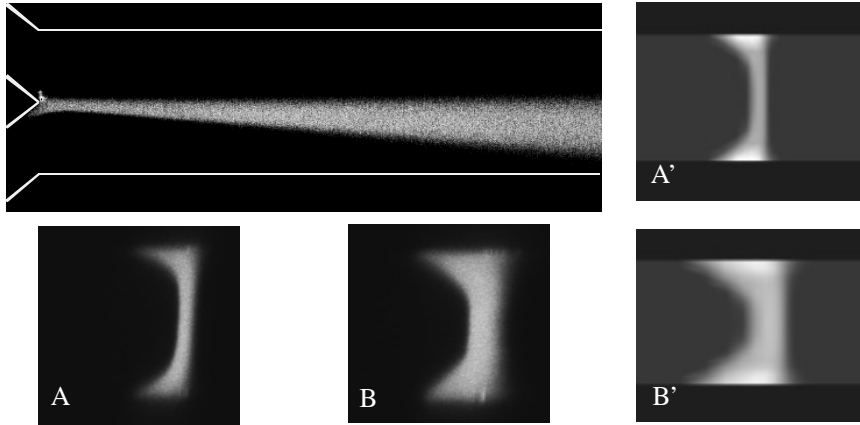


Figure 1: Experimental images from confocal microscopy (left). The corresponding simulated images (right) are qualitatively similar to the experimental images.

observing the concentration of this complex near the interface between flowing aqueous solutions of $5 \mu\text{M}$ fluo-3 and 1 mM CaCl_2 (Figure 1). At a given axial distance z from the point where the streams join, the diffusive mixing is more extensive (i.e. the fluorescent region is broader) in the slower-moving fluid near the wall of the channel than in the middle of the channel. At low flow velocities we observe some interdiffusion in the dead volume of the Y-junction (Figure 1), and we assume that its effect on the scaling behavior is negligible. There is also a pronounced asymmetry in the diffusion profile, because Ca^{2+} has a higher diffusivity ($D = 1.2 \times 10^{-9} \text{ m}^2/\text{s}$) than fluo-3 ($D = 1.0 \cdot 10^{-10} \text{ m}^2/\text{s}$) and because of the differences in concentrations of CaCl_2 and fluo-3.

To test the theoretical predictions, we analyzed experimental data with Scion Image. We smoothed the 512×512 pixels images of fluorescence (such as shown in Figure 1) corresponding to $100 \times 100 \text{ mm}^2$ xy scans before the analysis. For a given x (on each image we analyzed images only near $x = 0$ and near $x = H/2$) the width $d(z)$ of the region mixed by diffusion was taken to be the width of the fluorescent region with the intensity above 0.2 of the maximum intensity. The spreading $d(z)$ was always sufficiently small to be in a flow with uniform velocity profile in the y -direction.

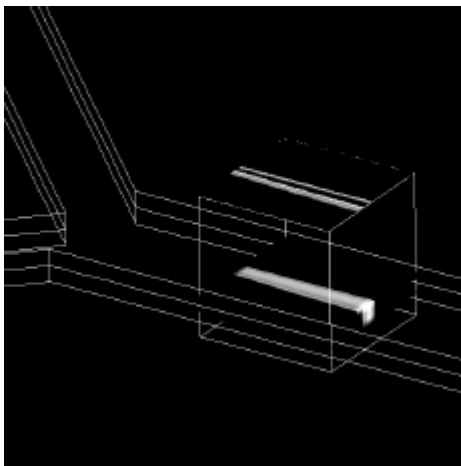


Figure 2: Standard fluorescent microscopy experiments effectively integrate in the vertical direction.

IV. Numerical Analysis

Numerical analysis can be a valuable tool for the design of microfluidic systems. Once anchored by experimental results, numerical results can predict the operation of the device over a range of parameters and geometries. Numerical analysis was performed using FlumeCAD [5]– an integrated design tool that enables the design and modeling of complex microfluidic devices. The Y-mixer was modeled by solving the incompressible Navier-Stokes equation for the velocity and pressure fields. The steady-state velocity field was then used in the coupled solution of three species transport equations – two reagents and one product. In

order to compare with the experimental results, the effective rate for the binding reaction was assumed to be infinite. The concentration of all three species was assumed to be dilute, so that the properties of the carrier were constant. The above equations were solved using a fully three-dimensional finite element based CFD engine.

Many experiments are performed using standard fluorescent microscopy techniques, which have the effect of integrating the three dimensional fluorescent signal in the vertical direction (as in figure 2). This obscures the effect of the three dimensional diffusion profile. Using numerical integration, the effective diffusive widths that would be seen with standard microscopy techniques were calculated.

V. Results

Confocal microscopy was used to measure the diffusive width at a sequence of locations in the channel, for a maximum flow rate of 16 cm/s. Results shown in figure 3 agree well with theoretical predictions. In the center of the channel, where the flow is uniform, the width scales as the $1/2$ power of the distance down the channel. Near the wall, the scaling behaves as the $1/3$ power of distance. Experiments were also performed at several flow rates, and the results are shown in figure 4. The diffusive width scales as the $-1/2$ power of flow rate in the center of the channel, and as the $-1/3$ power of flow rate near the channel wall, which is in agreement with theoretical predictions.

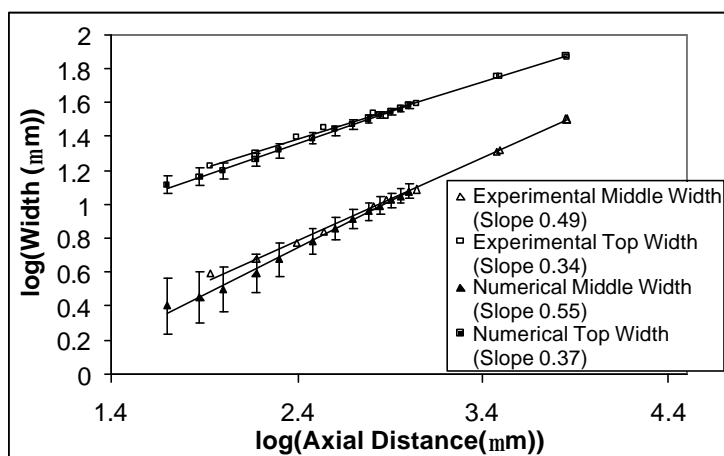


Figure 3: Experimental and numerical results for average flow velocity 8 cm/s.

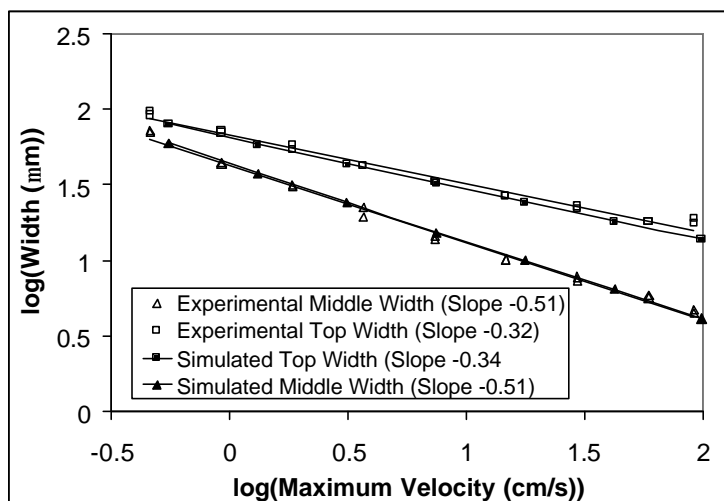


Figure 4: Experimental and numerical results at several flow rates. Widths were measured 500 mm downstream from the intersection.

Numerical simulations agree well with the experimental results. The distribution of the fluorescent compound at two positions in the channel compares qualitatively with the experimental results (Fig. 1), and the simulations also predict the same scaling laws for diffusive width as a function of axial distance and flow rate (Figs. 3,4).

Vertical integration of the three-dimensional simulated results, to mimic a standard microscopy setup, gives some interesting results (see figure 5). The scaling of the diffusive widths with distance depends on the threshold used. With a lower threshold (20%), the width scales roughly as the $1/3$ power of distance. However, as the threshold is raised toward 80%, the scaling law approaches the $1/2$ power of distance. This interesting result can be explained by figure 6. The layer near the wall, where the $1/3$ power scaling takes place, is thin for the flow regimes investigated here (this can be visualized from experimental and numerical images, figure 1). A line plot of intensity across the

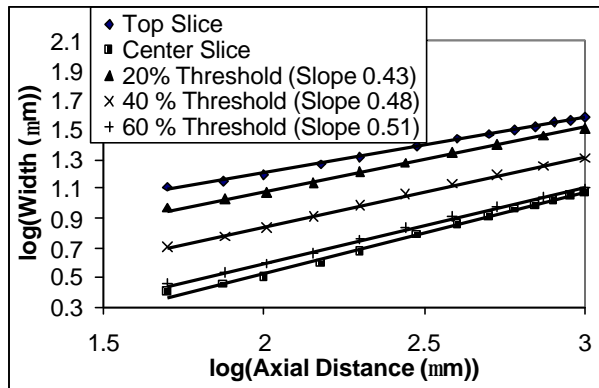


Figure 5: Diffusive widths measured with standard microscopy setups depend on the threshold used.

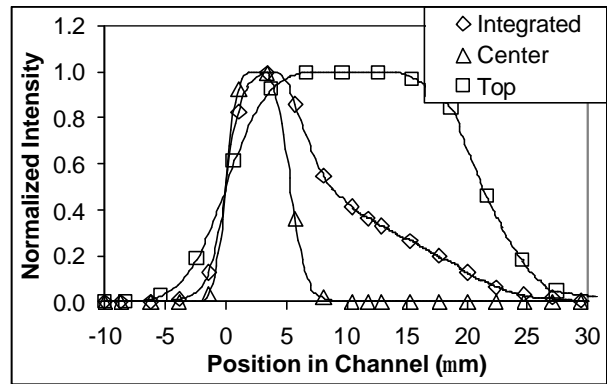


Figure 6: Fluorescence profiles 500 mm from the intersection. The shape of the integrated peak explains the effects of the different thresholds.

channel shows that this results in a wide base on the peak shape (figure 6); so a lower threshold effectively gives the width in the shear layer. As the threshold is raised, the total amount of fluorescence in the shear layer drops below the threshold, so the 1/2 power scaling from the center of the channel is recovered.

VI. Conclusions

Both experimental and numerical results agree well with theoretical predictions for the behavior of diffusive layers in pressure driven flow. The results demonstrate that three-dimensional effects can be important for the operation of devices using this type of diffusion. If uniform velocity diffusion scaling laws are applied blindly, device performance may not be as expected.

Numerical results have provided some additional insight that may help to design laminar flow mixing devices more accurately. When using a standard confocal microscopy detection system, the use of a high threshold for peak width calculation can ensure that the desired width scaling with distance is achieved.

Acknowledgments

This work was funded by the DARPA Composite CAD program, under FlumeCAD (Grant no. F30602-98-2-0151) and NetFlow (Grant no. F30602-96-2-0306).

References

- [1] A. E. Kamholz, B. H. Weigl, B. A. Finlayson and Paul Yager, "Quantitative Analysis of Molecular Interaction in a Microfluidic Channel: The T-Sensor", *Analytical Chemistry* **71**, pages 5340-5347, 1999.
- [2] A. Manz, F. Bessoth and M. U. Kropp, "Continuous Flow Versus Batch Process – a Few Examples", *uTAS '98 Conference Proceedings*, 235-240, 1998.
- [3] P. J. A. Kenis, R. F. Ismagilov and G. M. Whitesides, *Science* **284**, 83 (1999).
- [4] R.F. Ismagilov, A. D. Stroock, P.J.A. Kenis, H.A. Stone and G.M. Whitesides, "Experimental and Theoretical Scaling Laws for Transverse Diffusive Broadening in Two-Phase Laminar Flows in Microchannels", submitted to *Physical Review Letters*.
- [5] M. Deshpande, K.B. Greiner, B.F. Romanowicz, J.R. Gilbert, P.M. St John and T. Woudenberg, "CAD Analysis of PCR Well Containment", *MSM '99 Conference Proceedings*, pages 350-354, 1999.